



## CHAPTER II

### THEORETICAL BACKGROUND

#### 2.1 Poly (ethylene terephthalate) or PET

PET is usually produced by a condensation polymerization of dimethyl ester of terephthalic acid and ethylene glycol [1]. The PET structure containing aromatic ester units is shown in Fig. 2.1.

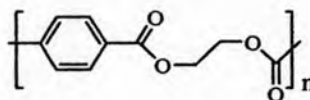


Fig. 2.1 The PET structure.

PET has many advantages such as good mechanical strength, toughness, polishing, fatigued resistance at elevated temperature and high melting temperature. Therefore, it is used in various industries such as textile industries, food and drink container, and biomedical devices. Some physical constants of PET are shown in Table 2.1.

The PET has excellent chemical and physical properties of the bulk. Moreover, it is inexpensive and easy to process, but it is not appropriate in some application. Since it has less hydrophilicity, it is modified for improving hydrophilicity by various modification techniques which are discussed in the next section.

Table 2.1 Physical constants of PET [1]

Properties	Value
<b>Glass Transition Temperature (<math>T_g</math> °C)</b>	
Amorphous	67
Semi-crystalline	81
<b>Melting Temperature (<math>T_m</math> °C)</b>	
commercial PET	250-265
<b>Degradation Temperature (<math>T_d</math> °C)</b>	
commercial PET	≈ 345
<b>Refractive index (Na light)</b>	
Amorphous, 25 °C	1.58
Crystalline and biaxially oriented, 23 °C	1.64
<b>Surface Tension (mN/m)</b>	
solid/liquid (25 °C)	39.5
<b>Tear Strength (film (g/m))</b>	
Initial, 23 °C	$23.6 \times 10^6$
propagating, 23 °C	$0.59 \times 10^6$
<b>Tensile Strength, MPa (<math>N/mm^2</math>)</b>	
PET film, 23 °C	172

## 2.2 Surface modification techniques

The modification can improve the value of PET products and create suitable properties for each application. As a result, the modification techniques are the important process for various industries. In recent years, the modification has been improved in developing surface treatment only without affecting the bulk properties because it needs to keep the excellent bulk properties [6]. In general, the surface modification of PET was modified by physical and chemical treatments [5, 7-8]. The physical treatment includes various methods such as flame treatment, plasma or corona treatment, irradiation treatment and electron beam treatment. The chemical

treatments are divided into two main types; wet treatment and surface grafting. These treatments have been purposed to resolve problems associated with undesirable properties of polymer. The hydrophobic property of PET is an important problem in some application such as cloth in textile industries and biocompatible devices.

The hydrophilic surface of PET is extensively modified by physical and chemical treatments. From the study of previous literatures [5, 9-12], the physical and chemical treatments use flame treatment, plasma or corona treatment, UV treatment, and laser treatment. These techniques have specific advantages and disadvantages.

Flame treatment can produce oxygen-containing functional groups. It is widely used in polyolefin [5]. PET can be treated by using high temperature at short treatment time (0.2-0.3 s). Flame treatment can be applied at high level, easy to process and low cost of operation. However, the flame treatment process is difficult to control in various materials.

Corona and plasma treatment [5, 13-14] are used in many industries and interested in various researches. The corona was produced from a corona discharge in ambient atmosphere by using high energy electromagnetic field. Thus, it can create oxygen-containing functional group at the surface. Corona treatment is used in continuous process which is suitable for industries. However, it needs high technology, while the operation cost is high. The plasma treatment utilizes similar principle as corona treatment. Plasma was generated by gas feeding in high energy electromagnetic field under a vacuum condition. Recently, this technique is mostly interested for many researches because it can selectively modify the surface with different gas feeding. However, it needs high technology. The operation cost is high while difficult to control the process in real application.

UV treatment [5-6, 9, 12] is a modification technique which is widely used for the polymer treatment. Photons from UV light are used to activate photolysis reaction and involved in the other reaction such as photo-oxidation reaction and photo-hydrolysis. UV treatment can be induced degradation under the present or absent of oxygen group at the PET surface. This phenomenon depends on wavelength of UV light. UV irradiation with the present of oxygen-containing functions such as carboxylic group and hydroxyl group has been exploited to enhance hydrophilic property at the surface or hydrophilicity. The UV technique has low operation cost

and is a clean technology. Moreover, it can be applied in continuous process, but it may affect the deeper layer.

The wet treatment [5] uses strong chemicals (acid or base) to react and change functional group of PET surface. The technique can be improved hydrophilicity at the surface, but it uses toxic chemicals in process.

Surface grafting [5, 8] employs chemical reaction to initiate a polymerization reaction to form a covalent bond of suitable macromolecular chain to polymer surface. The surface grafting can selective graft various polymers on the surface. However, it uses toxic chemicals and multi-staged process. Some techniques are summarized and shown in Table 2.2.

Table 2.2 Properties of hydrophilic modification techniques

Properties	Hydrophilic modification techniques			
	Plasma	Corona	Chemical	UV transmission
Low cost operation	No	No	Yes	Yes
Environmental friendly	Yes	Yes	No	Yes
Continuous process	Yes	Yes	No	Yes
Functional selection	Yes	No	Yes	No
Ambient atmospheric condition	No	Yes	Yes	Yes
Unchanged bulk properties	Yes	Yes	No	No

The UV treatment technique is an interesting technique for hydrophilic modification due to low cost of operation, easy to operate for continuous process. It also used non-toxic chemicals. However, the technique has problems because it may affect surface layer and deeper layer of material. That can be changed the bulk properties of PET.

## 2.3 UV evanescent field theory

### 2.3.1 UV radiation

UV light is an electromagnetic radiation, which can be represented as polarization, oscillation of electric and magnetic field that propagate in space [15]. The electromagnetic radiation composes of electric field and magnetic field that are orthogonal to each other and to the propagated direction. The magnetic field and electric field with respect to the direction of propagation of electromagnetic radiation are shown in Fig. 2.2.

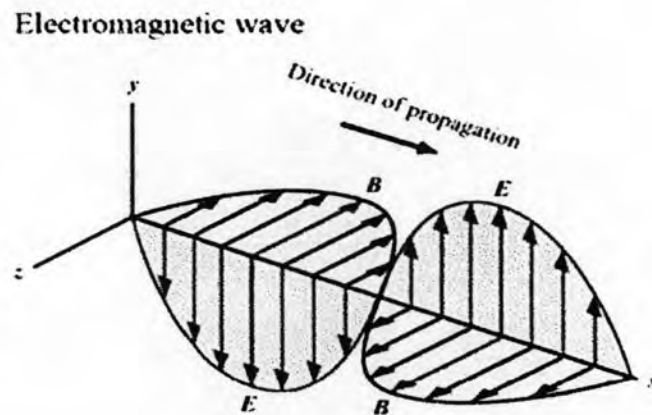


Fig. 2.2 The electromagnetic radiation propagates in space. Both electric and magnetic fields oscillate together, but perpendicular to each other while normal to the propagation direction.

In general, the UV light has wavelength in the range 20-400 nm [16-17]. The UV radiation is divided into three ranges: UVA (320-400 nm), UVB (280-320 nm) and UVC (< 280 nm). When an UV radiation is irradiated on a material, it affects the structure of materials. The UV radiation can create the energy level of chemical bond through the absorption. This phenomenon induces changes in the molecular structure (i.e., degradation and transformation). The changes depend strongly on wavelength, intensity, and irradiation times.

### 2.3.2 Reflection and refraction of light

When an electromagnetic radiation impinges an interface between two media with different refractive indexes, refraction and reflection occur. In the case of specular reflection, the angle of incidence equals the angle of reflection. When the electromagnetic radiation travels from the first medium to the second medium which has different refractive indexes, the propagation direction of radiation is changed from that of the incident radiation as shown in Fig. 2.3.

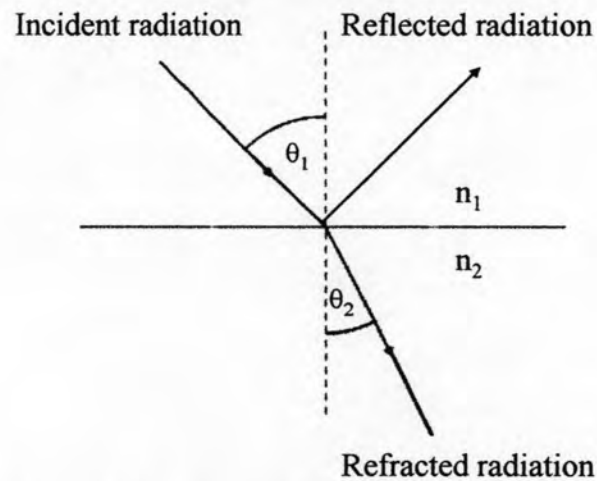


Fig. 2.3 Reflection and refraction of radiation at the interface.

The change of propagation direction follows Snell's law [15].

$$n_1 \sin \theta_1 = n_2 \sin \theta_2 \quad (2.1)$$

where  $n_1$  and  $n_2$  are refractive indexes of medium I and medium II, respectively,  $\theta_1$  and  $\theta_2$  are the angles of incidence and refracted angle, respectively.

Total internal reflection (TIR) is referred to a phenomenon where an electromagnetic radiation traveling within a denser medium impinges at the surface of a rarer medium with angle of reflected beam ( $\theta_2$ ) equals 90 degrees. The angle of incident initiates total internal reflection is called 'critical angle ( $\theta_c$ )'. The critical angle is illustrated in Fig. 2.4 and is calculated by equation 2.2.

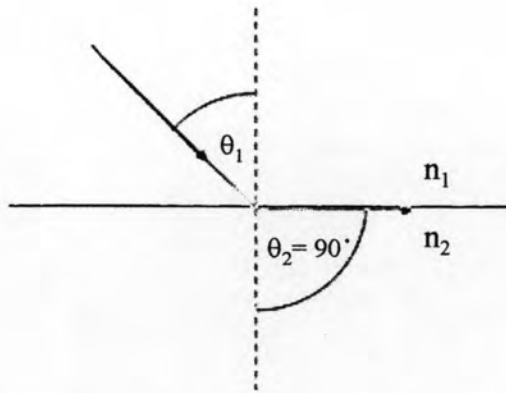


Fig. 2.4 Total internal reflection at the interface.

$$\theta_c = \arcsin(n_2 / n_1) \quad (2.2)$$

When the angle of incident beam exceeds the critical angle, the radiation totally reflects and cannot propagate to the second medium. However, the electromagnetic field is still present at the interface. The field is defined as an *evanescent field*.

### 2.3.3 Principles of total internal reflection

The total internal reflection (TIR) process can be discussed by the basis of Maxwell's equation [18]. The coordinate system model is divided into three coordinates as  $x$ ,  $y$  and  $z$ . The  $z$ -coordinate is the direction of thickness, while  $x$  and  $y$  lie on the interface between two media, as shown in Fig. 2.5.

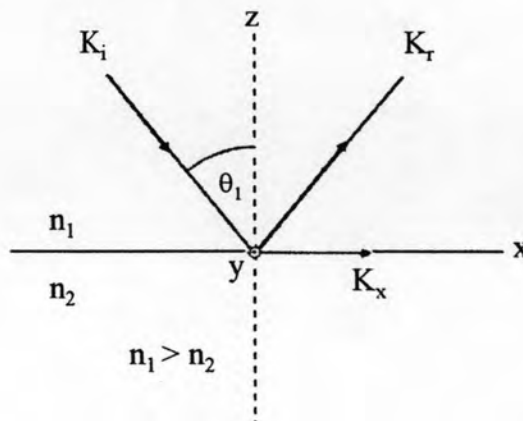


Fig. 2.5 Model of the system for total internal reflection.

The incident, reflected and transmitted wave vector are referred as  $K_i$ ,  $K_r$  and  $K_x$ , respectively. The wave of incident plane contains the electric ( $E^i$ ) and magnetic field ( $H^i$ ). Under this condition, the field is represented by two terms: s and p polarizations. The s (senkrecht) and p (parallel) polarizations are referred to transverse electric field (TE) and transverse magnetic field (TM), respectively. These fields are followed equation 2.3 [18].

$$E_p = E_x e_x + E_z e_z \text{ and } E_s = E_y e_y \quad (2.3)$$

The equation (2.3) is applied for the field at the interface of two semi-infinite distinct media. This field is obtained in the case of the incident beam is presented within the first medium of amplitude  $E_s^i$  and  $E_p^i$  contained within the  $z = 0$  plane. In the following equation, the x dependence and the time dependence are in the form  $\exp(-jx n_1 (\omega / c) \sin \theta)$  and  $\exp(j\omega t)$ , respectively with  $j = (-1)^{1/2}$

$$E_x = \frac{(2 \cos \theta)(\sin^2 \theta - n^2)^{1/2}}{(n^4 \cos \theta + \sin^2 \theta - n^2)} E_p^i \exp(-j(\delta_p + \pi / 2)) \quad (2.4)$$

$$E_y = \frac{2 \cos \theta}{(1 - n^2)^{1/2}} E_s^i \exp(-j\delta_s) \quad (2.5)$$

$$E_z = \frac{2 \cos \theta \sin^2 \theta}{(n^4 \cos \theta + \sin^2 \theta - n^2)} E_p^i \exp(-j\delta_p) \quad (2.6)$$

where  $n = n_2 / n_1$ , while

$$\delta_p = \arctan \left( \frac{(\sin^2 \theta - n^2)^{1/2}}{n^2 \cos \theta} \right) \quad (2.7)$$

$$\delta_s = \arctan \left( \frac{(\sin^2 \theta - n^2)^{1/2}}{\cos \theta} \right) \quad (2.8)$$

The intensity of electric field at  $z = 0$  depends on the incidence angle. The maximum field intensity is observed at the critical angle, (Fig. 2.6).



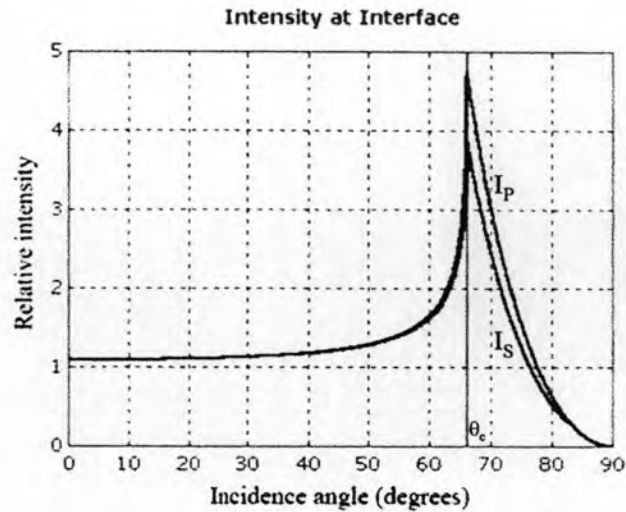


Fig. 2.6 The electric field intensity of p and s polarizations at the interface as a function of the incident angle ( $n_1=1.46$  and  $n_2=1.33$ ).

The depth dependence of electric field can be expressed in terms of angle of incidence as shown in equation 2.9 and 2.10.

$$E_p(z) = E_p^i \frac{(2 \cos \theta) \exp(-z/d_p)}{\cos \theta + j(\sin^2 \theta - n^2)^{1/2}} [-j(\sin^2 \theta - n^2)^{1/2} e_x + \sin \theta e_z] \quad (2.9)$$

$$E_s(z) = E_s^i \frac{(2 \cos \theta) \exp(-z/d_p)}{\cos \theta + j(\sin^2 \theta - n^2)^{1/2}} e_y \quad (2.10)$$

### 2.3.4 Interaction between electromagnetic radiation and matter under total internal reflection

The second medium can be divided into two types as non-absorbing medium and absorbing medium. The refractive index of the second medium can be expressed by equation 2.11 [19].

$$\hat{n}_2(\nu) = n_2(\nu) + ik_2(\nu) \quad (2.11)$$

where  $\hat{n}_2(\nu)$ ,  $n_2(\nu)$ , and  $k_2(\nu)$  are complex refractive index, refractive index and absorption index at frequency  $\nu$ , respectively

For a non-absorbing medium (i.e.,  $k_2(\nu) = 0$ ) [19-22], there is no reflection loss due to absorption while the reflection equals unity. The condition under this phenomenon is called the total internal reflection phenomenon. When a medium is absorbing (i.e.,  $k_2(\nu) > 0$ ), the electromagnetic radiation can be absorbed by the medium. Thus there is reflection loss due to the absorption by the absorbing medium. This phenomenon is called the attenuated total reflection (ATR) phenomenon as shown in Fig. 2.7.

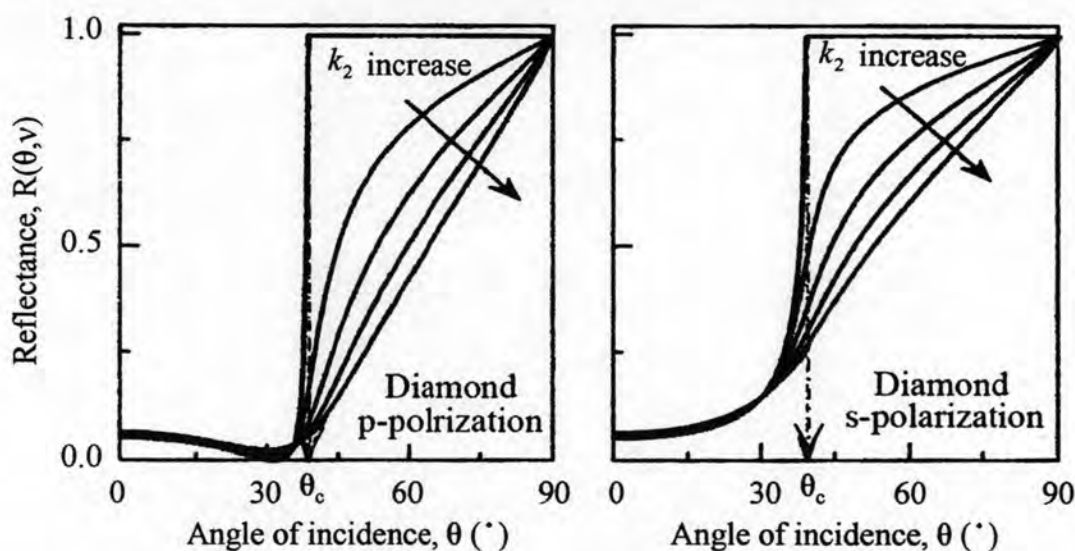


Fig. 2.7 Reflectance at various absorption indices as a function of angle of incidence with diamond as the IRE at  $\nu = 1000 \text{ cm}^{-1}$ ,  $n_1 = 2.4$ ,  $\hat{n}_2(\nu) = 1.5 + ik_2(\nu)$  and  $k_2(\nu) = 0.0, 0.1, 0.2, 0.3,$  and  $0.4$  respectively.

Although the electromagnetic radiation under total internal reflection cannot be traveled across the interface, there is a strong electric field at the interface of absorbing medium. The interaction between the electric field and the absorbing medium is the cause of reflection loss in ATR spectroscopy. The magnitude of that interaction depends on the properties of material (such as the complex refractive index of the absorbing medium and the refractive index of the internal reflection element) and experimental parameter (such as angle of incidence and polarization of incident beam). The intensities of absorbed and reflected beams in ATR are related by equation 2.12.

$$A(\theta, \nu) = 1 - R(\theta, \nu) \quad (2.12)$$

where  $A(\theta, \nu)$  and  $R(\theta, \nu)$  are absorptance and reflectance, respectively. The absorptance can be given in terms of the character of material and experiment parameter as:

$$A(\theta, \nu) = \frac{4\pi\nu}{n_1 \cos \theta} \int_0^\infty n_2(\nu) k_2(\nu) \langle E_z^2(\theta, \nu) \rangle dz \quad (2.13)$$

where  $\langle E_z^2(\theta, \nu) \rangle$  is the *mean square evanescent field* (MSEvF) at depth  $z$ . The MSEF decays exponentially as a function of distance from the interface. The MSEvF is expressed in terms of the field amplitude at the interface and its decay constant by:

$$\langle E_z^2(\theta, \nu) \rangle_{k=0} = \langle E_{z=0}^2(\theta, \nu) \rangle_{k=0} e^{-2z/d_p(\theta, \nu)} \quad (2.14)$$

where  $d_p(\theta, \nu)$  is the penetration depth and  $\langle E_z^2(\theta, \nu) \rangle$  and  $\langle E_{z=0}^2(\theta, \nu) \rangle$  are the MSEF at the depth  $z$  and at the interface, respectively. The decay profile of MSEF is decreased as the exponential function as the distance from the interface is increasing as shown in Fig. 2.8.

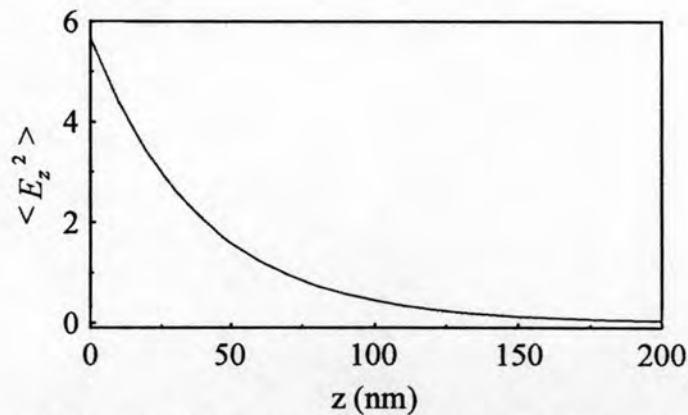


Fig. 2.8 The MSEF and its decay characteristics at  $\lambda = 365$  nm,  $\theta = 45^\circ$ ,  $n_1 = 2.417$  and  $n_2 = 1.58$ .

The penetration depth is defined as the distance from the interface where the evanescent field strength decays to  $1/e$  of its value at the interface. The penetration

depth depends on character of materials and experimental parameters and can be calculated by the following equation [23]:

$$d_p = \frac{\lambda}{2\pi n_1 [\sin^2 \theta - (n_2/n_1)^2]^{1/2}} \quad (2.15)$$

where  $\theta$  is the angle of incidence,  $\lambda$  is the wavelength of the radiation and  $n_1$ ,  $n_2$  are the refractive index of the first medium and the second medium, respectively. From the equation 2.15, the amplitude of evanescent field depends on various parameters such as wavelength, refractive indexes, and the angle of incident beam. In case of UV radiation, the evanescent field is penetrated at nanometer level from the interface between medium I and medium II (89.2 nm at 365 nm,  $\theta = 45$  degree,  $n_{diamond} = 2.417$  and  $n_{PET} = 1.58$ ). The penetration depths of UV evanescent fields at difference wavelength are shown in Table. 2.3

Table.2.3 The penetration depth of UV evanescent field at various wavelength with  $\theta = 45^\circ$ ,  $n_1 = 2.417$  and  $n_2 = 1.58$ )

$\lambda(nm)$	200	225	250	275	300	325	350	375	400
$d_p(nm)$	48.9	55.0	61.1	67.2	73.3	79.4	85.5	91.6	97.7

In the case of a weakly absorbing medium, the strength of the MSEF is slightly smaller than that of the non-absorbing medium. Under such a circumstance, the MSEF can be accurately estimated from the reflectance by the following equation.

$$\langle E_z^2(\theta, \nu) \rangle \approx \frac{1+R(\theta, \nu)}{2} \langle E_z^2(\theta, \nu) \rangle_{k=0} \quad (2.16)$$

When the equation 2.12 and 2.16 are substituted into equation 2.13, equation 2.17 is obtained.

$$2 \left[ \frac{1-R(\theta, \nu)}{1+R(\theta, \nu)} \right] \approx \frac{4\pi\nu}{n_1 \cos \theta} \int_0^\infty n_2(\nu) k_2(\nu) \langle E_z^2(\theta, \nu) \rangle_{k=0} dz \quad (2.17)$$

The above relationship can be simplified and the absorbance can be given by equation 2.34

$$A(\theta, \nu) \approx \frac{4\pi\nu}{\ln(10)n_1 \cos \theta} \int_0^\infty n_2(\nu)k_2(\nu) \langle E_z^2(\theta, \nu) \rangle_{k=0} dz \quad (2.18)$$

or

$$A(\theta, \nu) \approx \frac{2\pi\nu n_2(\nu)k_2(\nu)d_p(\theta, \nu) \langle E_{z=0}^2(\theta, \nu) \rangle_{k=0}}{\ln(10)n_1 \cos \theta} \quad (2.19)$$

The equation 2.18 can only be applied for weakly absorbing medium. However, this equation is the most convenient form for expressing the quantitative analysis between intensity of ATR spectral and material characters under experimental conditions where low absorption is observed.

### 2.3.5 Application of evanescent field irradiation

The evanescent field under the total internal reflection can be applied for surface characterization technique of materials. The technique is called attenuated total reflection Fourier transform infrared spectroscopy (ATR FT-IR). The technique is highly sensitive for surface characterization. In recent years, the evanescent field is also used for photo-polymerization [24]. The photo-polymerization by the evanescent waves or PEW is a photolithography process that is suitable for the fabrication of very thin films.

## 2.4 Diamond internal reflection element (Diamond IRE)

The internal reflection element (IRE) is an important component for ATR experiment. The IRE can transmit the desired electromagnetic radiations such as infrared and ultraviolet. The diamond is an appropriating material for UV radiation under ATR because it has suitable refractive index for ATR condition ( $n_{diamond} = 2.417$  as measured by sodium light at 589.3 nm) and can transparent UV radiation [25-26]. The diamond can increase the contact with sample medium due to its strength. Moreover, it can also used for ATR FT-IR characterization. The round brilliant cut diamond is needed for ATR condition. The facet of round brilliant cut

diamond has appropriated arrangements and proportions for ATR measurement. The diamond design depends on the refractive index of diamond, which is responsible for its brilliance (the amount of incident light that reflected to the observer). Commonly, the target of brilliant cut is achieved the total internal reflection by assessing the suitable *crown angle* and *pavilion angle*. The originally round brilliant cut of diamond was known as Tolokowsky's cut, which contains 34 degrees of *crown angle* and 41 degrees of *pavilion angle*. The Tolokowsky's diamond cut proportion showed in Fig. 2.9.

The critical angle between diamond ( $n_1 = 2.417$ ) and air ( $n_2 = 1.0$ ) equals 24.4 degrees. According to the Tolokowsky's cut proportion, the total internal reflection takes place because the incident angle of light is greater than the critical angle. When the second medium is an absorbing medium such as polymer  $n_2 = 1.5$  (the critical angle equals 38.4 degrees), the incident angle at the pavilion facet remains greater than the critical angle. Therefore, diamond is suitable as an IRE.

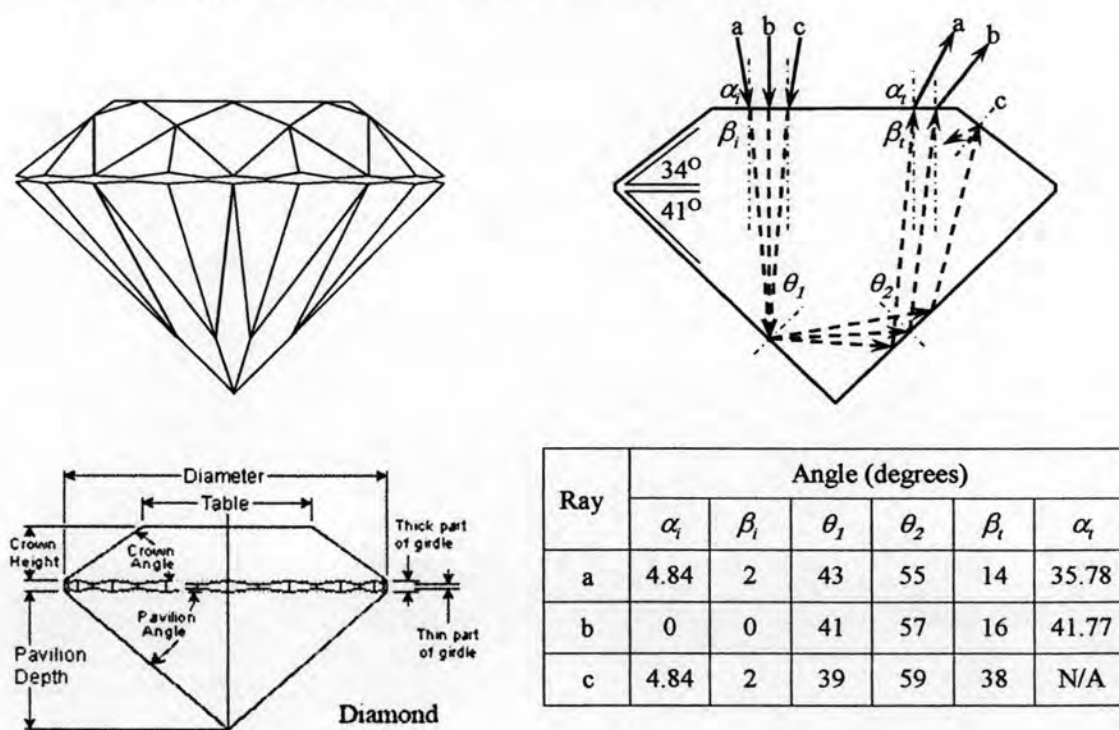


Fig. 2.9 A round brilliant cut of diamond based on Tolokowsky's diamond cut proportion and a summary of angle of incidence at the pavilion facet.

## 2.5 Polymer degradation

The polymer degradation can be induced by various processes such as thermal, biological, photo-oxidative, chemical, hydrolytic, mechanical, thermo-oxidation and photolysis degradations [27-31]. In general, the polymer degradation is a harmful process, which should be avoided or prevented. The degradation process can be led to the change of physical and chemical properties of polymer. However, polymer degradation may be useful in some processes. The depolymerization of polymer can be leading to the generation of highly pure monomer for other processes. Moreover, the degradation process can be applied in polymer modification.

### 2.5.1 Photo-degradation of PET

The PET is widely used in many industries. The photo-degradation by UV light is an important process that involving absorbed light, electronic excitation and energy transfer of PET [6, 28, 30-31]. When a suitable radiation is irradiated in the sample, the molecules are excited from ground state to the excited state. If the lifetime of excited state is sufficiently long, the species can be participated in many chemical transformations such as isomerization, dissociation and decomposition. Normally, the PET contains the carbonyl group of ester. The excited carbonyl groups are decomposed following two types of Norrish reactions. Norrish type I reaction is a radical cleavage between carbonyl group and  $\alpha$ -carbon atom. The reaction gives carbon monoxide product. The Norrish type II reaction occurs through the intermediate of six member ring. The hydrogen atom from  $\gamma$ -carbon is abstracted to oxygen atom of ester and simultaneously  $\beta$ -scission cleavage without radical reaction. Both Norrish type I and II reactions are presented in Fig. 2.10.





$$I_0 = I_R + I_S + I_T + I_A \quad (2.20)$$

where  $I_0$  is the intensity of the incident beam and  $I_R$ ,  $I_S$ ,  $I_T$  and  $I_A$  are the intensities of reflected, absorbed, scattered and transmitted beams, respectively.

When a specimen is inserted between light source and detector, the specimen can interact with the radiation. Generally, the attenuated and non-attenuated intensities of radiation are interested in the measuring instrument. The proportional ratio of the specimen is related to the chemical compositions as the Beer-Lambert's law given in equation 2.21

$$I_0 / I = e^{-A(\nu)} = e^{-c_2 \varepsilon(\nu) l} \quad (2.21)$$

where  $A(\nu)$  is the absorbance of sample at wavenumber ( $\nu$ ),  $c_2$  and  $\varepsilon(\nu)$  are the concentration of absorbing functional group, the wavenumber-dependent extinction coefficient and film thickness, respectively.

From the Beer-Lambert's law, both extinction coefficient and absorbance are the functions of the wavenumber, thus it can be quantitatively analyzed.

Generally, a simple transmission experiment is widely used in the analysis. It provides spectral information of the sample which is related to chemical structure and chemical composition. The simple transmission technique is not suitable for surface analysis. Moreover, it cannot be employed for spectral acquisition of opaque samples. As a result, the reflected radiation and scattered radiation are employed for surface analysis and opaque samples. The ATR FT-IR and FT-Raman are the spectroscopic techniques for the measurement of the internal reflected radiation and scattered radiation, respectively.

### 2.6.1 ATR-FTIR spectroscopy

ATR FT-IR is a surface sensitive technique which measures the internal reflected radiation. This technique can be acquired the spectra of sample surface. Moreover, it has various advantages which is non-destructive, quick and easy sampling, high accuracy and high resolution with the quantitative analysis in various

scales [15]. In the ATR FT-IR configuration, IRE is infrared transperence and has high refractive index. The IRE is optically contacted with lower refractive index medium (sample). The infrared light is coupled into the IRE with the angle of incidence greater than the critical angle. When the sample molecules interact with a suitable infrared radiation, it can be partially absorbed the infrared radiation. The molecule which is changing the vibrational energy level and dipole moment can provide the molecular information. The molecular information is related to the functional groups, and molecular structure. The internal reflected beam which is relating with the absorbance (equation 2.12) is detected by the detector. The ATR FT-IR configuration is shown in Fig. 2.12.

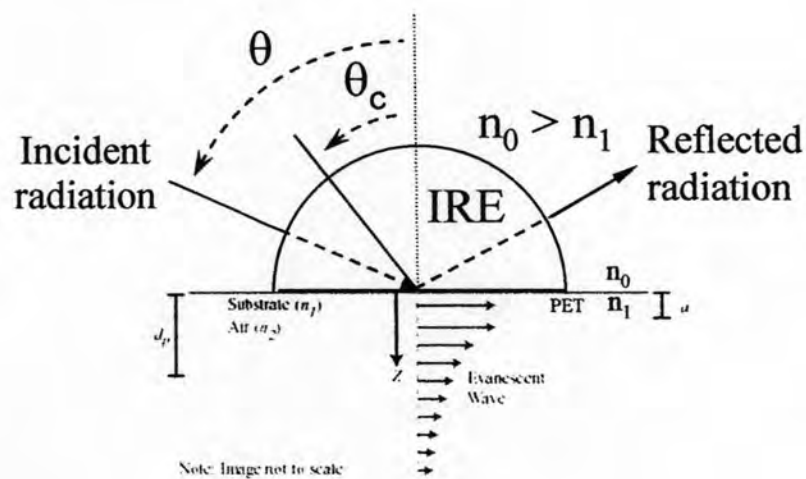


Fig. 2.12 ATR FT-IR configuration.

### 2.6.2 FT-Raman spectroscopy

FT-Raman spectrometer measures the scattered radiation of the molecule which can be changed the polarizability [33-34]. When a sample is irradiated with monochromatic radiation ( $\nu_0$ ) that cannot be absorbed by the sample. A fraction of incident radiation is scattered in all directions. The scattering process explained in terms of photon collision from incident light consisting elastic scattering and inelastic scattering (Raman Effect). In the case of elastic scattering, the photon energy is

unchanged ( $\nu = \nu_0$ ; Rayleigh scattering). The changing energy occurs during inelastic collision ( $\nu \neq \nu_0$ ). The scattered process is discussed in Fig. 2.13

From Fig. 2.13, a molecule is excited from the vibrational ground state ( $\nu = 0$ ) into the higher level. The molecule which immediately goes back to the ground state does not change the photon energy. These photons remain in the original frequency (i.e., the Rayleigh scattering). If the molecule is excited and gone back to the lower state, which is not the ground stage ( $\nu = 1$ ), the photon energy after the collision will be reduced and called 'Stokes Raman scattering'. The molecule at  $\nu = 1$  is excited from the photon and gone back into the ground state. The scattering photon with higher energy is called 'Anti-Stokes Raman scattering'. The Stokes and Anti-Stokes Raman scattering are interested in Raman spectroscopy. Normally, the Anti-Stokes bands are obviously weaker than the Stokes, thus only the Stokes lines are recorded.

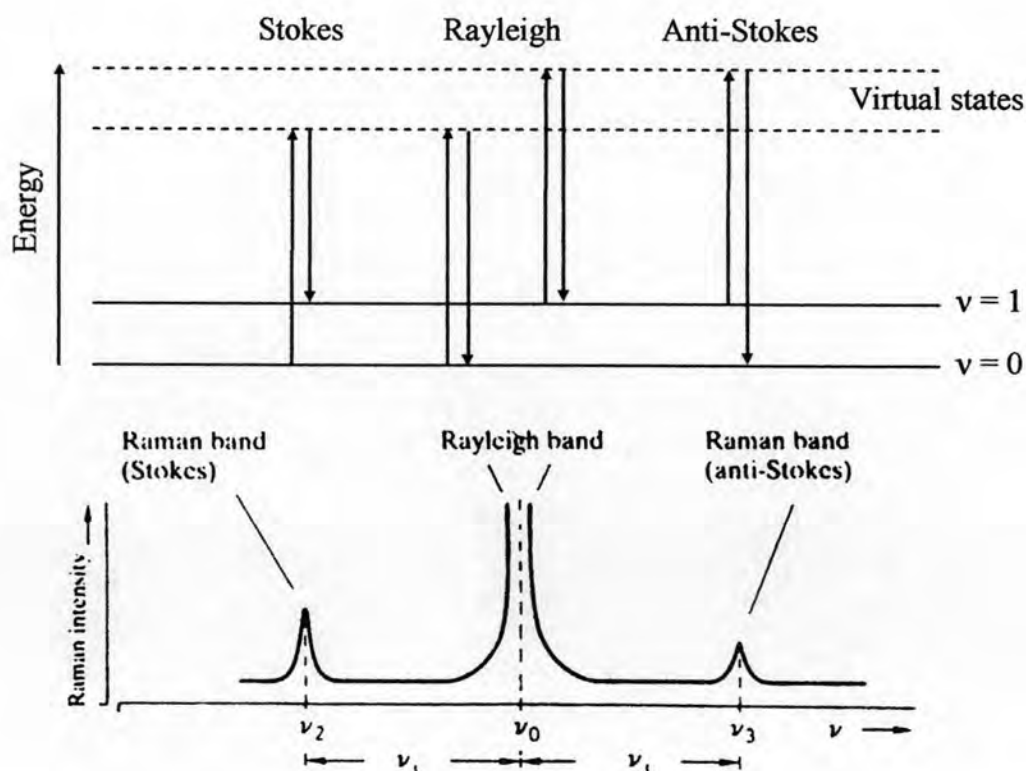


Fig. 2.13 The energy level processes of Raman scattering.

### 2.6.3 Comparison of Infrared and Raman spectroscopy

Both, IR and Raman spectroscopy give the molecular information. However, the IR and Raman spectra of the same specimen are not obviously similar. Since the IR spectroscopy gives molecular information of asymmetric molecules, which are changing the dipole moment upon vibration. The Raman spectroscopy gives the molecular information associated with the changing in polarizability upon vibration. When IR and Raman techniques are simultaneously employed, the complete molecular information is obtained. The major differences between IR and Raman techniques are summarized in Table. 2.4

Table 2.4 The major differences between IR and Raman techniques.

Title	Raman spectroscopy	Infrared spectroscopy
Sample limitation	Color; fluorescence	Single crystal; metals
Purge requirement	No	Yes
Interaction	Scattering	Absorption
Source	Laser (monochromatic radiation)	Blackbody radiation or diode laser (polychromatic IR radiation)
Frequency measurement	Relative with the excitation frequency	Absolute
Requirement for	Change of the polarizability (Symmetric molecules)	Change of the dipole moment (Asymmetric molecules)
Spectral representation	Intensity	Absorbance